Onboard Orbit Estimation with Tracking and Data Relay Satellite System Data

J.B. Dunham,* A.C. Long,† H.M. Sielski,‡ and K.A. Preiss‡
Computer Sciences Corporation, Silver Spring, Maryland

An investigation was performed to determine an appropriate estimation technique for onboard orbit determination using simulated data of the Tracking and Data Relay Satellite System (TDRSS). A summary of results is presented from studies done with an extended Kalman filter and a sliding batch differential corrector. These estimators were evaluated when used with both baseline and worst-case TDRSS measurement errors and with tracking configurations for two types of orbits: a high-inclination, near-circular orbit with an altitude of 700 km and a moderately inclined, lower altitude orbit. Each estimation result was evaluated by comparing the true ephemeris with the estimated ephemeris.

Introduction

IN support of an experiment at NASA Goddard Space Flight Center (GSFC) to demonstrate the feasibility of performing autonomous spacecraft navigation with data from the Tracking and Data Relay Satellite System (TDRSS), a prototype onboard orbit determination system for use with TDRSS data was developed. It combined hardware and software designed to simulate both the onboard and ground support processing.[1] As a part of that support, a study was made of onboard estimation accuracy and reliability with TDRSS data.

Using TDRSS data for onboard estimation will not require large hardware expenditures, since NASA will already be using TDRSS for ground-based satellite tracking and for relaying command and telemetry data. Therefore, TDRSS interfaces will already exist, and NASA spacecraft will be equipped with TDRSS transponders. The major constraint in the use of TDRSS is that only a limited number of users may use the forward link over a given time span, a condition that limits the frequency of tracking contacts.

The onboard orbit determination algorithm selected for use with the TDRSS data must be reliable and accurate. A summary of the results from two of the estimation techniques selected for study is presented here: an extended Kalman filter (EKF) and a sliding batch differential corrector (SBDC). Performance of the estimators was compared with respect to 1) accuracy using a nominal tracking schedule, 2) effect of reducing the tracking schedule, 3) effect of large TDRSS ephemeris errors, 4) accuracy in the presence of anomalous or deleted passes of data, and 5) effect of onboard frequency standard errors.

The EKF and the batch estimator studies described in this paper are presented in much more detail in Refs. 2-4. The work described here was carried out under Contract NAS 5-24300 using the capabilities of the Research and Development Goddard Trajectory Determination System (R&D GTDS) available at the time of the study.[5-7]

Estimators

This section describes characteristics of the EKF and SBDC which are relevant to the current study. These are standard estimators, as discussed in Ref. 8 and presented in many other texts. Details on the implementation of these estimators are given in Refs. 6 and 7. Information on the specific solve-for set and modeling is discussed later, under "Evaluation Results," with a summary presented in Tables 5 and 6.

Presented as Paper 81-0204 at the AAS/AIAA Astrodynamics Specialist Conference, Lake Tahoe, Nev., Aug. 3-5, 1981; submitted Oct. 7, 1981; revision received Dec. 21, 1982.

*Principal Engineer.
†Department Manager.
‡Member, Technical Staff.

EKF

The R&D GTDS FILTER program contains an EKF with a linear process noise covariance matrix model,

$$Q(t_k) = \dot{Q} \cdot (t_k - t_{k-1}) \tag{1}$$

where

$Q(t_k)$ = process noise
$\dot{Q}$ = diagonal matrix of constants that are the assumed noise variance rates of change for the solve-for parameter set
t_k = measurement time
t_{k-1} = measurement time of previous observation

The state covariance is augmented by $Q(t_k)$ at each measurement time t_k. In the current study, nonzero process noise rates of change were used for the velocity, clock drift, and drag parameters. The values used for $\dot{Q}$ were chosen by empirical studies in which a wide range of values was tried and the results compared to see what worked best. For the baseline Landsat-4 case, for example, values for the velocity components from 10^{-12} to 10^{-24} km^2/s^3 were tried, with 10^{-20} km^2/s^3 giving the best results. This is discussed in detail in Ref. 3.

Data editing is performed by comparing the observation residual to the residual predicted from the covariance and the observation measurement noise. If the ratio of the two is larger than a user-input editing threshold, the observation is deleted. The ith predicted observation residual w_i is computed as

$$w_i = (H_i P H_i^T + \sigma_i^2)^{1/2} \tag{2}$$

where

H_i = vector of partial derivatives of the observation with respect to the estimation parameters at time t_i
P = covariance matrix of the estimation parameters propagated to time t_i
σ_i = ith observation noise standard deviation

The ith observation is edited if

$$|Y_i| / w_i > V \tag{3}$$

where Y_i is the ith observation residual and V the editing threshold.

SBDC

The SBDC is a minor variant of the usual batch differential correction (DC) orbit determination process. The term "sliding" refers to the fact that the data span continues to slide forward, picking up a pass of new data and dropping off a pass of old data (where a pass of data is a set of data collected within a short time span). The orbital elements (but not the covariance) that were determined in a previous slide are propagated forward to serve as starting values for the next slide. A new solution then is attempted using these data.

The batch least-squares estimation DC program of R&D GTDS was modified as described in Ref. 3. The program was started with a span of data approximately 12 h in length, which, for the moderately close Earth orbits studied, contained 3-9 passes of data over 7-8 orbits. These data were used to estimate the satellite position, velocity state, and other parameters, as requested. In a typical run consisting of 12-h spans from a file covering 24 h, five separate DC program runs were made.

Both the data editing and the estimation convergence criteria of the SBDC depend on the root-mean-square (rms) observation residual, which is computed as

$$\text{rms} = \left(\frac{1}{N} \sum_{i=1}^{N} \frac{Y_i^2}{\sigma_i^2} \right)^{1/2} \tag{4}$$

where N is the total number of observations.

An observation was deleted if its residual, when scaled by the measurement standard deviation, was more than the editing factor times larger than the rms from the previous iteration. That is, if, for the ith observation,

$$\frac{(|Y|_i/\sigma_i)}{\text{rms}} > V \tag{5}$$

the observation was deleted. A record of the data edited was not saved; for each iteration, the editing process was repeated. In addition, each span was processed separately using an infinite a priori rms in the first iteration.

An individual DC of the SBDC was judged to have converged if the percentage of difference between the predicted rms (prms) and the rms fell below a convergence tolerance E. The prms was computed to predict the effects of the just-computed state update on the rms as

$$\text{prms} = \left[\frac{1}{N} \sum_{i=1}^{N} \frac{(Y_i - H_i x)^2}{\sigma_i^2} \right]^{1/2} \tag{6}$$

where x is the state update vector.

Measurement Models

The TDRSS is a system of three tracking and data relay satellites to be maintained in circular, near-equatorial, geosynchronous orbits. Two operational satellites, Tracking and Data Relay Satellite-East (TDRS-E) and TDRS-West (TDRS-W), will be spaced approximately 130 deg apart at 41° and 171°W longitude, respectively. The third will be a spare to be used if one of the operational satellites fails. The TDRSS is discussed in detail in Ref. 9.

Two tracking modes were studied for use in onboard orbit determination: one-way Doppler and two-way range and/or Doppler. The one-way Doppler measurements would be extracted onboard the user spacecraft from tracking signals originating on the ground, relayed through a TDRS, and received by the user spacecraft. One-way data would require only the forward link of the round-trip measurement that produces the two-way data. The accuracy of one-way data would be degraded by any error in the user frequency standard used to extract the Doppler measurements and to obtain the measurement time tags. The two-way data would be extracted and time tagged on the ground from the round-trip propagation of the tracking signals; the resulting data are collected and relayed back to the user spacecraft through the command link. The use of the Doppler measurement type was simulated by using the delta-range measurement type so that the existing R&D GTDS capabilities could be used.

Simulated Two-Way Range

The two-way range and delta-range observations was simulated as follows:

$$\begin{aligned} R(t_r) &= c(t_r - t_t) + R_b + \sigma_r \\ &= p(t_r) + R_b + \sigma_r \end{aligned} \tag{7}$$

where

c = speed of light
t_r, t_t = true receive and transmit times
R_b = range bias
σ_r = random range error
$p(t_r) = |R_{\text{TDRS}}(t_t) - R_{\text{USER}}(t_r)|$, the geometric range between TDRS and user
R_{TDRS} = TDRS position error
R_{USER} = user spacecraft position vector

Simulated Two-Way Delta-Range

The two-way delta-range observations were simulated as follows:

$$\Delta R(t_r) = p(t_r) - p(t_r - s) + \Delta R_b + \sigma_{\Delta R} \tag{8}$$

where

s = integration time to measure ΔR
ΔR_b = delta-range bias
$\sigma_{\Delta R}$ = random delta-range error

Simulated One-Way Delta-Range

The one-way delta-range observation simulation model was as follows:

$$\begin{aligned} \Delta R(t_r + \Delta t_r) = {} & p(t_r) - p(t_r - s) + c\{\dot{b}s + \ddot{b}s[t_r - (s/2)]\} \\ & + \Delta R_b + \sigma_{\Delta r} \end{aligned} \tag{9}$$

where

Δt_r = user clock error, $b + \dot{b}t + \tfrac{1}{2}\ddot{b}t^2$
b = clock bias
$\dot{b}$ = clock drift = oscillator frequency bias
$\ddot{b}$ = clock drift rate = oscillator frequency drift

Use of a polynomial to approximate clock error is discussed in Ref. 10, pp. 207-220. This is similar to the model used for a priori clock correction when processing Global Positioning System (GPS) data, as discussed in Ref. 11.

Estimator Computation Models

The observation models used in the estimators were the same as the simulation models without the addition of the range or delta-range bias and random errors.

Evaluation Procedure

Several programs available in R&D GTDS were used to evaluate the orbit determination accuracy. Figure 1 illustrates the evaluation procedure. The simulated data used by the estimator were supplied by the DATASIM program, which could corrupt the range and delta-range measurements with measurement errors and random measurement noise. The

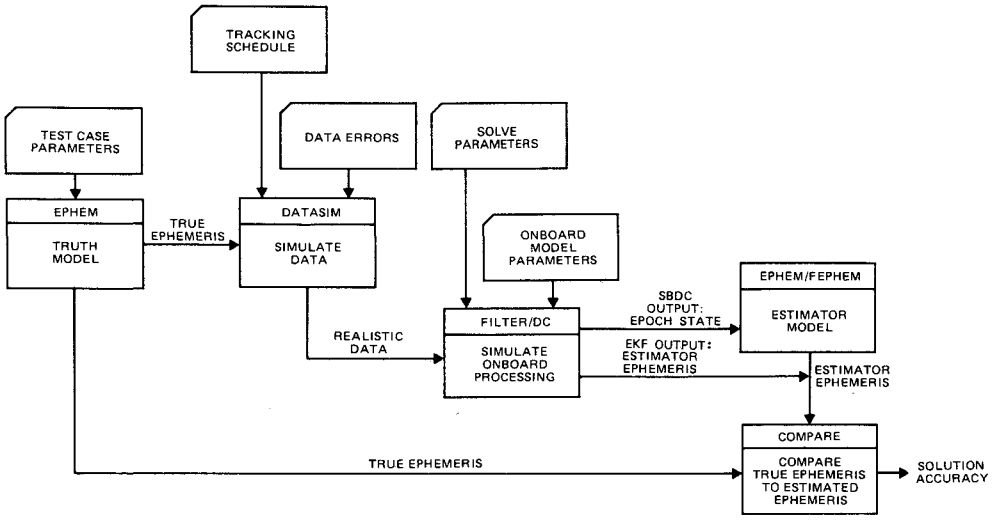

Fig. 1 Evaluation procedure for TDRSS study.

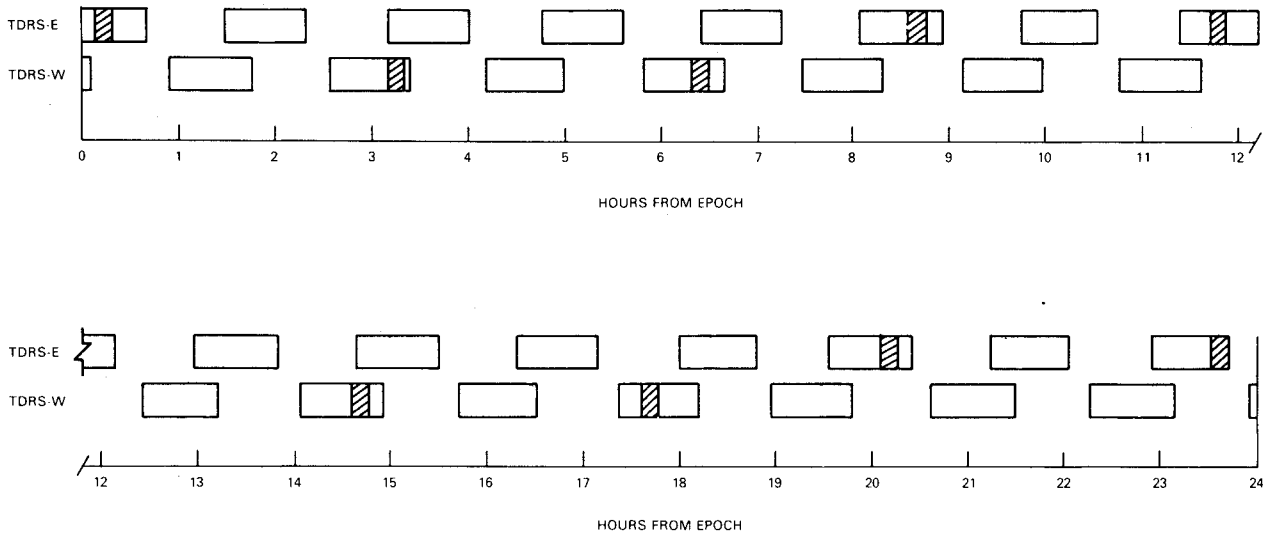

NOTES: 1. EPOCH : OCTOBER 1, 1980.

2. SHADED AREAS CORRESPOND TO ONE PASS PER TWO REVOLUTIONS DATA SET.

Fig. 2 Contacts for the every two-revolution case for GRO.

ephemeris of a "truth" model for the user satellite was compared with the ephemeris produced by the estimator. Deviations between the two ephemerides provided a measurement of the accuracy obtained by the estimator for a particular test case.

The time spans for comparing each estimator were chosen to cover times when an operational onboard estimator would be annotating data. In the case of the SBDC, this was a span covering at least one orbit, and possibly two, beyond the last data points. For the EKF, this comparison time span covered an orbit or more beyond the initial data. This time span should be one in which the transient effects of initializing the filter are not noticeable with the filter settled to a steady-state or equilibrium condition. Since it is of some interest to learn how long this settling process takes, two comparison spans were used: one at the midpoint and one at the end of the data.

Test Cases

The Landsat-4 and the Gamma Ray Observatory (GRO) spacecraft were selected as sample test cases for onboard orbit estimation. Landsat-4 has a near-polar inclination and a medium altitude, and GRO has a lower altitude and a less inclined orbit. Table 1 lists the Landsat-4 and GRO orbital elements and spacecraft parameters. The TDRSS satellites were placed in near-circular stationary orbits 130 deg apart with periods of 1436.2 min.

Table 1 Landsat-4 and GRO orbital elements, area, and mass

Parameter	Landsat-4	GRO
Epoch	Oct. 1, 1980	Oct. 1, 1980
Coordinate system	True of date	True of date
Semimajor axis, km	7086.901	6778.140
Eccentricity	0.001	0.0017
Inclination, deg	98.181	28.0
Longitude of ascending node, deg	354.878	0.0
Argument of perigee, deg	180.0	0.0
Mean anomaly, deg	0.0	0.0
Period, min	98.956	92.56
Area, m^2	20.0	20.0
Mass, kg	1700.0	1700.0

TDRSS Tracking Schedules

The TDRSS observation simulation determined the TDRSS visibility from the user spacecraft by testing to see whether the

TDRSS fell within the user antenna's field of view and was not occulted by the Earth. With an antenna modeled as a cone pointing along the radial direction with a half-angle of 100 deg, the time span of line-of-sight contact between Landsat-4 or GRO and any single TDRS was 40-60 min.

The baseline tracking schedule used in these studies was one in which the user satellite was tracked for one pass of data of 10-min duration by a TDRSS once per user-satellite orbit revolution. A set of range and/or delta-range measurements constituted a pass of data. The time between range and delta-range measurements and the delta-range computation interval was set at 10 s, yielding 30 delta-range measurements for every complete pass of data. For both measurement types combined, there were 30 range measurements and 30 delta-range measurements.

The effect of the length of time between subsequent passes of data was studied by decreasing the data contact to one contact every two or three user-satellite revolutions. For any given pass of data, the user satellite was restricted to tracking by only one TDRS. However, most simulations were run with alternating TDRS contacts on subsequent passes of data. Figure 2 shows the TDRS visibility for the GRO satellite and the location of the data passes used to simulate one tracking contact every other revolution.

Table 2 Data simulation measurement errors

Parameter	Baseline standard deviation One-way data	Two-way data
Random range error, m	–	1
Random delta-range error, cm	10	1
Range measurement bias, m	–	7
Delta-range measurement bias, cm	–[a]	–

[a] The delta-range measurement bias due to the user clock is as follows:
= 60,000 + 0.00035t cm for the accurate clock 2
= 60,000 + 0.0069t cm for the accurate clock 1
= 300,000 + 0.69t cm for the NASA standard transponder
where t is measured in seconds from the clock epoch.

Table 3
Data simulation TDRS ephemeris error model

Parameter	Value
Period of sinusoid, h	24
Radial amplitude H, m	35
Cross-track amplitude C, m	35
Along-track amplitude L, m	80
Along-track growth rate $\dot{L}$, m/day	250

[a] Sinusoidal period for radial, cross-track, and along-track TDRS ephemeris errors.

Measurement Error Models and Anomalous Data

The errors applied to the observation data were random errors applied to the measurement, biases applied to the range data, and errors in the TDRS ephemeris supplied to the estimator. The one-way data also had a frequency bias applied to the delta-range and a user-clock error applied to the observation time tag. The nominal values for the random measurement errors and range bias are listed in Table 2. Values selected for the TDRS ephemeris errors, presented in Table 3, were chosen based on the accuracies attainable for definitive orbit determination, as discussed in Ref. 12. The values used in simulating the user clock error are presented in Table 4. These are representative of a crystal oscillator (given as NASA standard transponder) and a cesium standard (accurate clocks 1 and 2).

To study the performance of the estimators in the presence of transitory data problems, data sets were created in which one or more 10-min passes of data were given anomalously large errors. In this way, the effects of transitory problems that are periodic or that create larger random errors or a bias on the data were studied.

Dynamic Modeling Errors

Dynamic modeling errors were simulated by a mismatch of the spacecraft acceleration model and frequency standard used in the data simulation with those used in the estimation. Physically, these errors arise from the lack of precise models, both for the accelerations acting on the spacecraft and for the behavior of onboard clocks. Dynamic modeling errors affect the accuracy of the propagation of orbital vectors and clock

Table 4 Data simulation quadratic user-clock model

Coefficient	One-way data: NASA standard transponder	One-way data: Accurate onboard clock 1	One-way data: Accurate onboard clock 2	Two-way data: Perfect clock
User-clock bias, s	0	0	0	0
User-clock drift, s/s	1×10^{-6}	2×10^{-7}	2×10^{-7}	0
User-clock drift rate, s/s/day	2×10^{-7}	2×10^{-9}	1×10^{-10}	0

Table 5 Dynamic models

Parameter	Data simulation value	EKF value	SBDC value
GM	398600.64, GEM-9	398600.80, GEM-1	398600.80, GEM-1
Geopotential	15×15, GEM-9	8×8, GEM-1	8×8, GEM-7
Resonance (GRO only)	Yes	No	No
Solar flux	150×10^{-22} W/m^2/Hz	200×10^{-22} W/m^2/Hz	200×10^{-22} W/m^2/Hz
Aerodynamic drag coefficient	2.0	2.2	2.2
Sun and moon	Yes	Yes	No
Solar radiation pressure	No	No	No
Integrator	Cowell 12th-order	Runge-Kutta 3(4+)	Cowell 12th-order

Table 6 A priori values and measurement standard deviations

Parameter	Baseline input value: One-way data	Two-way data
A priori state offsets		
X, Y, Z, m	100	100
$\dot{X}, \dot{Y}, \dot{Z}$, cm/s	30	30
A priori user clock parameters		
b (bias), s	0	–
$\dot{b}$ (drift), s/s		
NASA standard transponder	1.1×10^{-6}	
Accurate onboard clock	2.2×10^{-7}	–
$\ddot{b}$ (drift rate), s/s/day	0	–
A priori ρ_I	0.0	0.0
A priori standard deviations (EKF)		
X, Y, Z, m	316	316
$\dot{X}, \dot{Y}, \dot{Z}$, m/s	1.0	1.0
$\dot{b}$, s/s	1×10^{-6}	–
ρ_I (GRO only)	1.0	1.0
A priori standard deviations (SBDC)		
X, Y, Z	∞	∞
$\dot{X}, \dot{Y}, \dot{Z}$	∞	∞
$\dot{b}$	∞	–
ρ_I (GRO only)	∞	∞
Standard deviation of measurement error		
Range, m	–	40
Delta-range, cm	10	1

Table 7 Results for Landsat-4

Run No.	Estimator	Data type	Tracking schedule, rev	rms/max position deviation, m: 9-12 h	Typical 3-h prediction	21-24 h	Data error model
B5	EKF	2-way ρ, $\Delta\rho$	1	78/130	–	41/65	Baseline
L2	SBDC	2-way ρ, $\Delta\rho$	1	–	81/124	–	Baseline
L1	SBDC	2-way $\Delta\rho$	1	–	81/124	–	Baseline
L12	SBDC	2-way ρ, $\Delta\rho$	2	–	95/155	–	Baseline
EL1	EKF	2-way ρ, $\Delta\rho$	3	508/793	–	203/313	Baseline
L25	SBDC	2-way ρ, $\Delta\rho$	3	–	123/259	–	Baseline
E4	EKF	2-way ρ, $\Delta\rho$	1	41/85	–		8*H*, 8*C*
L15	SBDC	2-way $\Delta\rho$	1	–	187/262	–	8*H*, 8*C*, TDRS ephemeris update
O4	EKF	2-way ρ, $\Delta\rho$	1	66/95	–	140/228	Anomalous data at 13 h: ρ error = 7 km $\Delta\rho$ error = 300 cm
SL1	SBDC	2-way $\Delta\rho$	1-2	–	127/226	–	Baseline
M4	EKF	1-way $\Delta\rho$	1	282/418	–	87/169	Accurate clock 1
SL2	SBDC	1-way $\Delta\rho$	1-2	–	175/290	–	Accurate clock 2
EL2	EKF	1-way $\Delta\rho$	1-2	172/271	–	38/66	Accurate clock 2
SL3	SBDC	1-way $\Delta\rho$	3	–	141/213	–	Accurate clock 2

state vectors. The dynamic models used in the truth model and in the estimators are given in Table 5. The Goddard Earth models 1, 7, and 9 used in the various satellite force models are presented in Refs. 13-15. Both the EKF and SBDC used the GEM-1 value for the central body term, GM. In a 24-h period, the differences between the SBDC dynamic model and the truth model produce an along-track deviation of 1.2 km for Landsat-4 and 26.6 km for GRO. The primary source of error is the difference in GM between the truth and estimator models.

Baseline Parameters

The estimation vector selected was the minimum required to achieve adequate estimation of the user-satellite trajectory. The satellite state, the frequency bias for the one-way case, and the drag parameter for the GRO case were estimated. Table 6 lists the a priori offsets (initial state errors) or values, the a priori standard deviations associated with the estimated parameters, and the measurement noise standard deviations that were used in the baseline runs.

Evaluation Results

Representative results taken from the EKF and SBDC studies with the Landsat-4 and GRO satellites are shown in Tables 7 and 8, respectively. These cases have been extracted from Refs. 2-4, which contain a large number of test cases and a more detailed discussion of the procedures and results.

The runs are grouped to allow comparison of the performance of an extended sequential estimator with a batch processor. Statistics for the extended sequential estimator are given for two periods: 9-12 and 21-24 h after the beginning of the data spans. The later period is to assess the estimator accuracy unaffected by transients associated with initializing the estimator. For some runs, the differences between the 9-12-h span and 21-24-h span show that the extended sequential estimator has not reached an equilibrium solution at 12 h. In

Table 8 Results for GRO

Run No.	Estimator	Data type	Tracking schedule, rev	rms/max position deviation, m: 9-12 h	Typical 3-h prediction	21-24 h	Data error model
P12	EKF	2-way ρ, $\Delta\rho$	1	141/234	–	60/80	Baseline
G2	SBDC	2-way, ρ, $\Delta\rho$	1	–	252/420	–	Baseline
G1	SBDC	2-way $\Delta\rho$	1	–	252/420	–	Baseline
EG1	EKF	2-way ρ, $\Delta\rho$	3	508/793	–	203/313	Baseline
G25	SBDC	2-way ρ, $\Delta\rho$	3	–	412/680	–	Baseline
Q17	EKF	2-way $\Delta\rho$	1	173/315	–	109/194	$4\dot{L}$
G6	SBDC	2-way $\Delta\rho$		–	245/380	–	$4\dot{L}$
T3	EKF	2-way $\Delta\rho$	1	162/248	–	226/379	Anomalous data at 13 h: $\Delta\rho$ error = 300 cm
G19	SBDC	2-way $\Delta\rho$		–	693/896	–	
R8	EKF	1-way $\Delta\rho$	1	306/453	–	129/235	Accurate clock 1
SG1	SBDC	1 way $\Delta\rho$		–	208/283	–	Accurate clock 1
SG2	SBDC	1-way $\Delta\rho$	1	–	167/303	–	Accurate clock 2
SG3	SBDC	1-way $\Delta\rho$	1	–	20049/27398	–	NASA standard transponder
EG2	EKF	1-way $\Delta\rho$	3	384/744	–	235/626	Accurate clock 2 plus random clock noise
EG3	EKF	1-way $\Delta\rho$	3	34575/62193	–	37137/57478	NASA standard transponder

the case of the SBDC estimator, the statistics are associated with a typical ephemeris prediction that uses an initial state derived from processing data spanning the previous 12 h.

Two-Way Data Results

Effects of the Baseline Data Errors

Statistics are given in Table 7 for EKF run B5 and for SBDC runs L1 and L2 for the Landsat-4 case. Table 8 shows results for the GRO data: EKF run P12 and SBDC runs G1 and G2. The baseline data sets with a pass of two-way data every revolution gave comparable results whether both range and delta-range or only delta-range data were used.

The decrease in estimated ephemeris accuracy resulting from an increase in the dynamic modeling error during the prediction span is clearly seen in the GRO SBDC results in G1 and G2 as compared with the Landsat results in L1 and L2. The EKF was less affected by this increase, as seen from comparing runs P12 and B5, since the data processed during the comparison spans kept the EKF estimated ephemeris error from accumulating. The error in the along-track direction for Landsat-4 B5 EKF run is shown in Fig. 3. The behavior of these errors was characteristic of the EKF, in which a large initial deviation (reaching, in this case, a maximum of 2549 m) was reduced to an acceptable level as the data processing proceeded and the filter achieved an equilibrium solution. For comparison, the along-track error for the L1 SBDC run is shown in Fig. 4. In this case, Fig. 4a is a plot of the solution error over the data span, and Fig. 4b shows the error in the trajectory predicted beyond the data span. These errors behaved in a manner characteristic of a DC estimator, in which the solution errors over the data arcs have a mean of zero.

Effect of Reduced Data Sets

Results are presented for a data pass every two revolutions (L12) and every three revolutions (EG1, G25, EL1, and L25). Using data at the two-revolution spacing did not significantly affect the solution accuracy. When the data spacing was further increased, the solution accuracy was degraded. For the SBDC, runs G25 and L25 show the rms error nearly double that of runs G2 and L2, which had data every revolution. The effect on the EKF was to increase the rms by a factor of more than 3 and to increase the time required for the EKF to reach an equilibrium, as seen by comparing run EL1 with B5 and run EG1 with P12.

Effect of TDRS Ephemeris Errors

It was found that the estimators performed almost as well when only delta-range data were used as when both range and delta-range data were used, as long as the weighting on the range data properly reflected the larger error in that data type from the TDRS ephemeris errors. When the TDRS ephemeris errors were not reflected in the range measurement noise (that is, when the estimator assumed a more accurate measurement than was available), the estimation accuracy was degraded. Proper use of the range data requires a good knowledge of the level of error in the TDRS ephemeris, a factor that increases the risk of using that data type. Examples of increased ephemeris errors are given with runs E4, L15, Q17, and G6.

SBDC run L15 also included the effect of a TDRS ephemeris update 14 h after the beginning of the Landsat-4 data set. In this case, the first two data spans of the SBDC were processed with increasing TDRS ephemeris errors. As the SBDC processed successive 12-h spans, the level of the total TDRS ephemeris error decreased. The rms of the predicted solution is 202 m for the second span and 139 m for the fifth; the maximum deviations are 304 and 190 m, respectively. The statistics given in Table 7 are from the first data span.

Effect of Anomalous Data

Data sets were generated in which one or two passes had anomalous data errors, that is, large increases in any or all of the error sources beyond what was expected by the estimators. If the estimator could recognize that such a data pass was in error and edited it, there was virtually no effect on the solution accuracy. If the estimator did not recognize that the data pass had larger errors, then its inclusion corrupted the solution accuracies. These cases were of more interest than those in which the data errors were so large that bad data were successfully edited. Run O4 is one for which a comparison of the results with EKF run B5 shows a degradation of the solution accuracy from the biased data pass. Not all of the Landsat-4 data with anomalous errors were edited.

In the GRO cases with anomalous data (runs T3 and G19), the errors are also such that not all of the anomalous data were edited. The bad data pass for run G19 had a significant effect on the second span of the SBDC, but the estimator recovered by the fourth span. The statistics given in Table 8 are those for the second span; for the fourth, they are 377 m rms and 566 m maximum deviation.

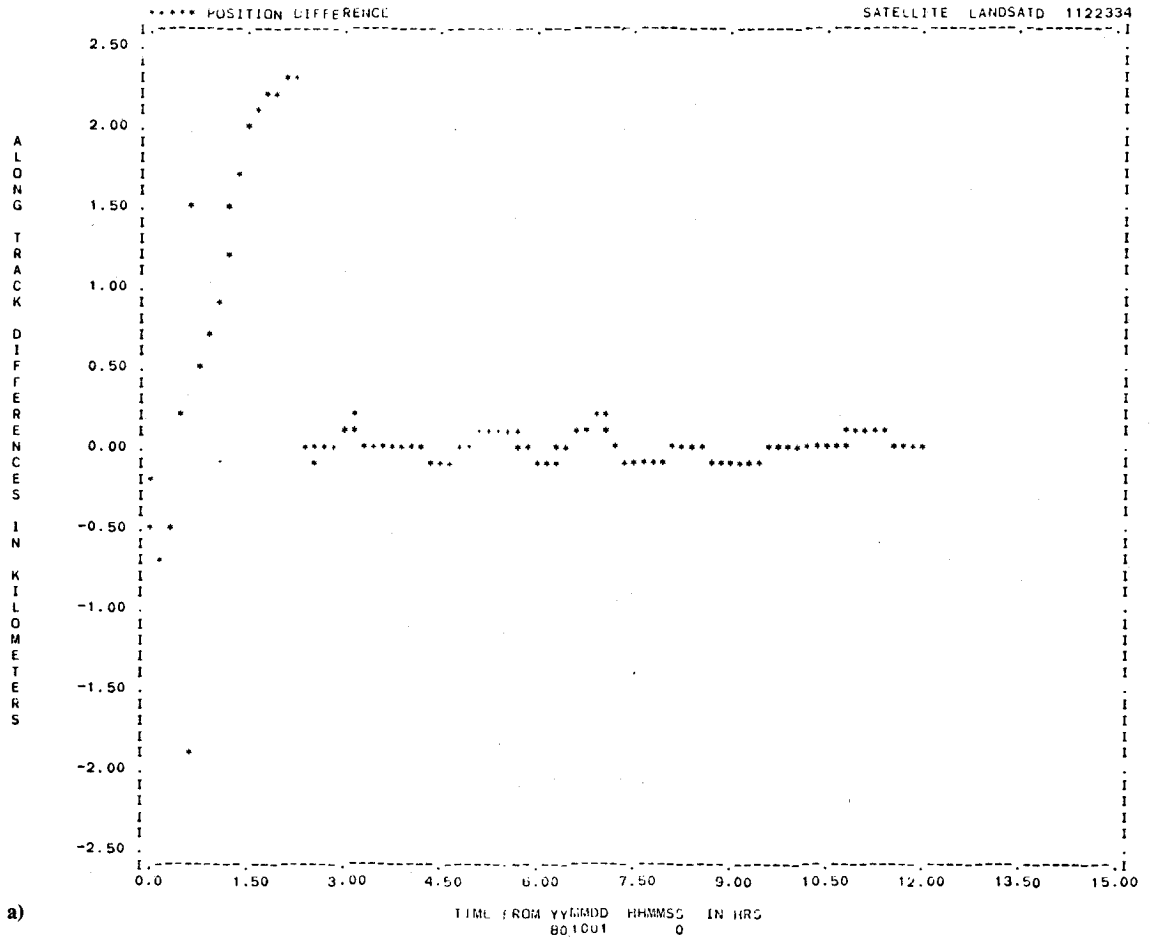

a)

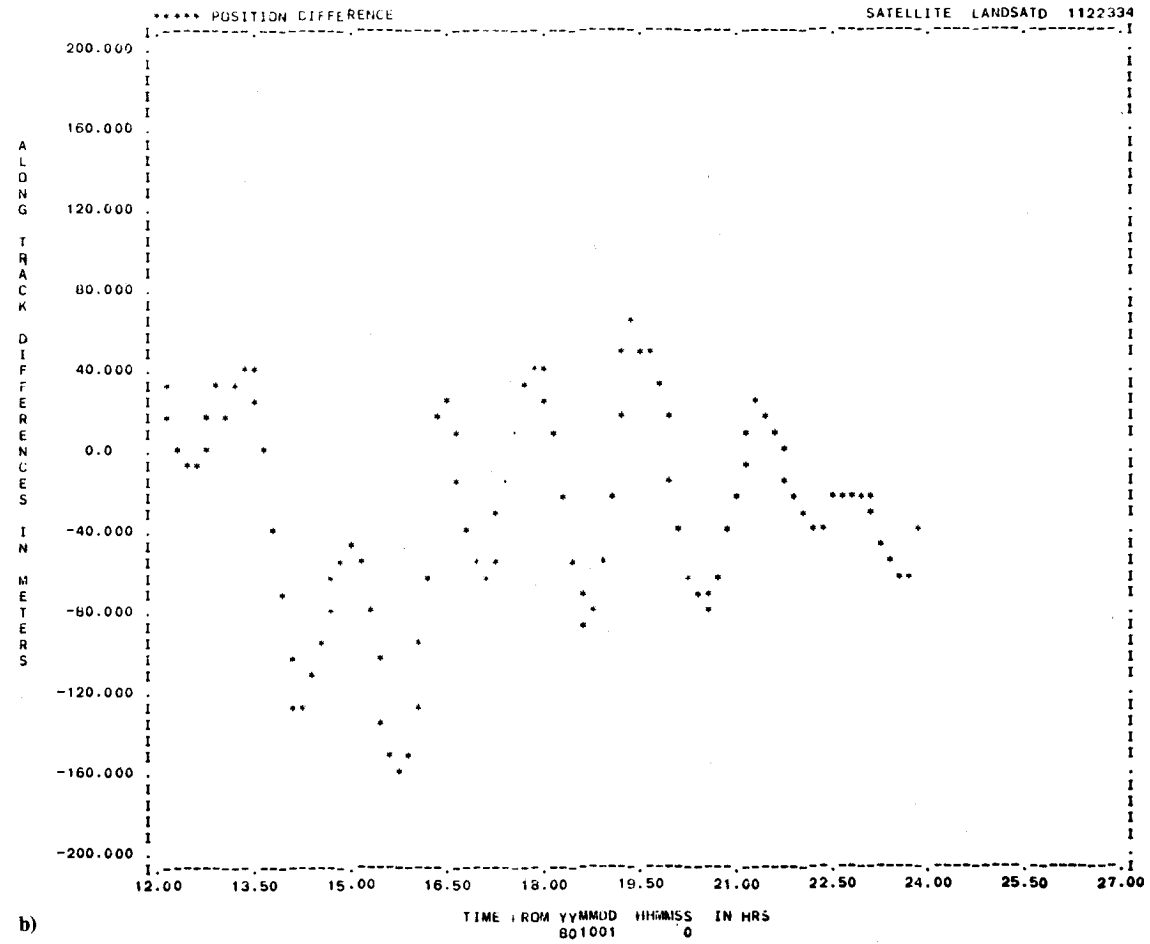

b)

Fig. 3 Along-track error for EKF run B5.

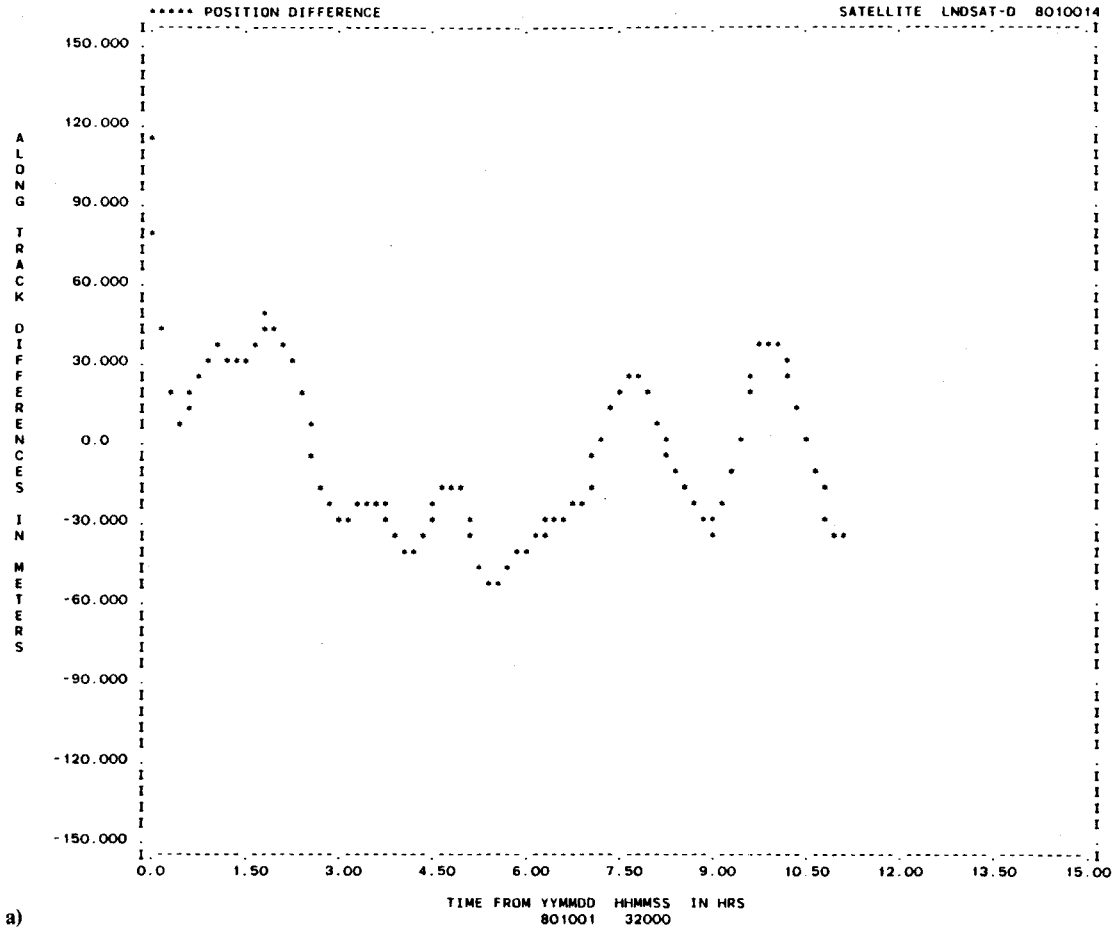

a)

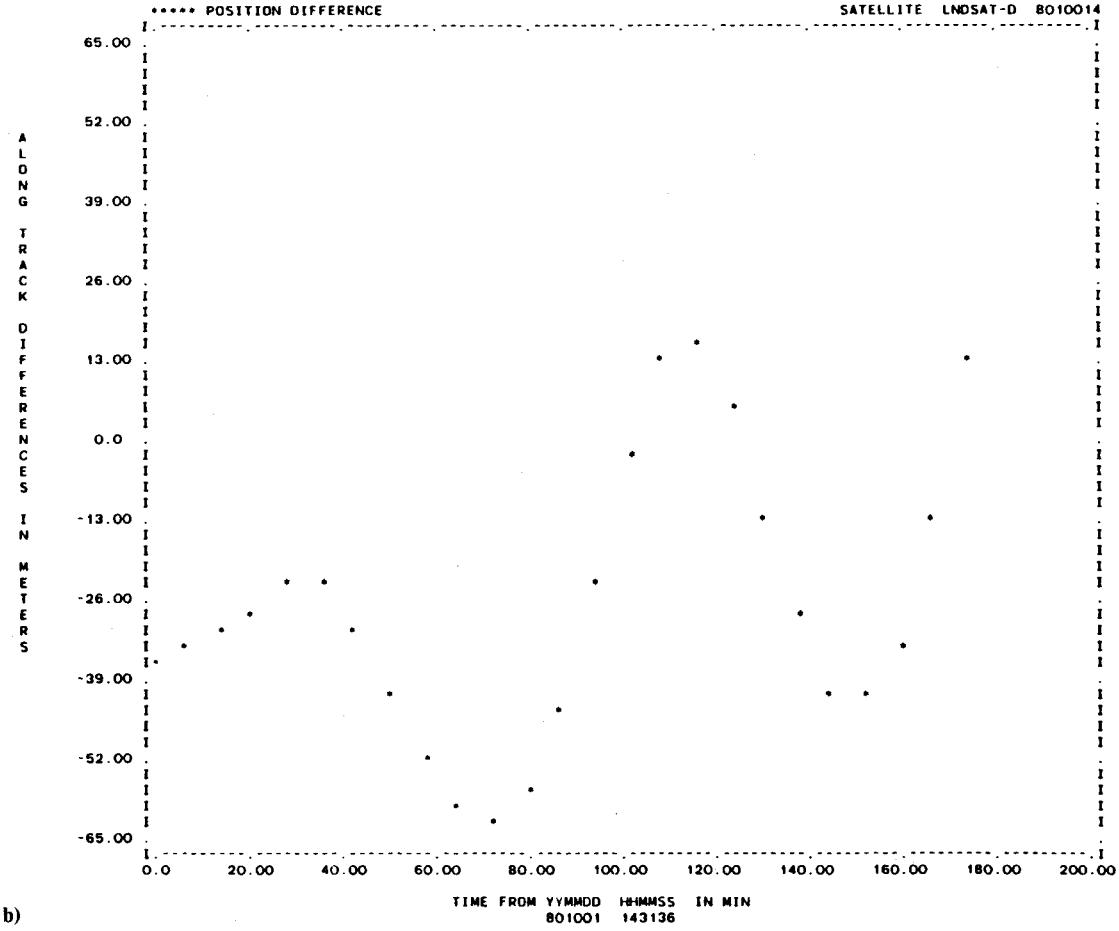

b)

Fig. 4 Along-track error for SBDC run L1.

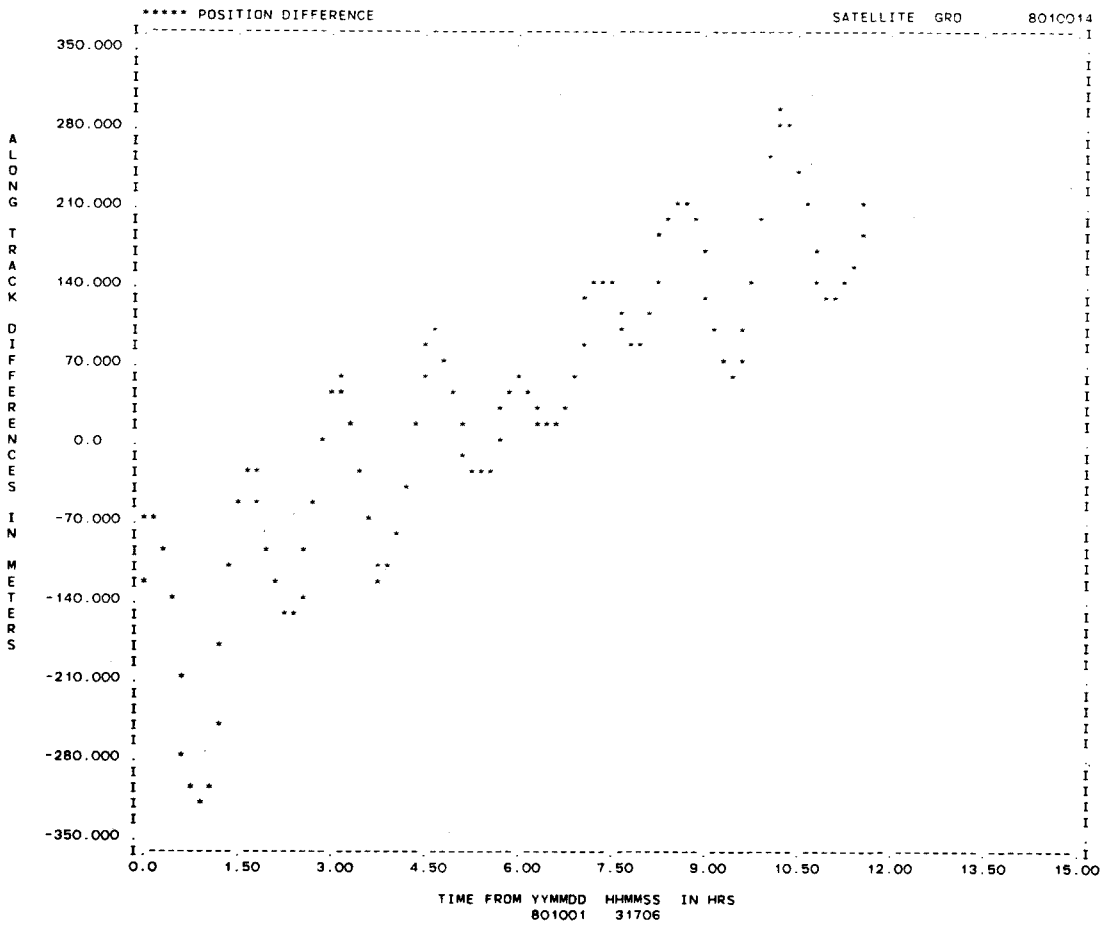

Fig. 5 Along-track error for SBDC run SG1.

Effect of Poor Tracking Geometry

A data set with missing passes of one TDRS was devised in such a way that, during the second 12 h, data were available every other revolution, and all but one of the data passes were from the same TDRS. Case SL1 was an SBDC run that used these data. This run had results of an accuracy similar to L25, which used data with a better distribution. It was found that, for two-way tracking, use of poor geometry with baseline data errors had an effect no worse than reduced tracking.

One-Way Data Results

Effect of Baseline Data Errors

The use of the one-way data degraded the solution accuracy as compared with the use of two-way data. This phenomenon occurred because of the additional errors introduced by the onboard clock timing and frequency errors and the higher random measurement noise level. To account for the timing errors, the clock drift term was estimated in the one-way case.

The EKF required a longer processing span to achieve an equilibrium solution than the two-way data, but the EKF could follow the changing frequency bias. The SBDC attempted to model the bias as a constant over a 12-h time span when it is, in fact, linearly increasing. The SBDC SG1 plot of the definitive solution along-track errors shown in Fig. 5 illustrates the result with the errors containing a linear term. The effect was least for the clock with the least error. The results from the run SG2 estimation with the most accurate clock are comparable to run G1 with two-way data.

Replacing the accurate oscillators in the one-way data model with the NASA standard transponder, the frequency drift of which was two to three orders of magnitude larger, produced much worse results. As seen in run SG3, the errors in the SBDC grew to tens of kilometers when attempting to model this oscillator as one with a constant frequency bias. When both the frequency bias and the drift were estimated, the solutions were as accurate as with the two-way data. However, this should not be construed as demonstrating that the frequency drift must be estimated for accurate solutions. It is simply a demonstration of the need for correctness in the estimator modeling of one-way data since the data were simulated with the same oscillator used in the estimator.

Effect of Reduced Data Sets

Using less data affected the solution accuracy no more for the one-way data cases than it did for the two-way data cases. Run SL3 of the SBDC, for example, gave results similar to those of L25. Both runs used data spaced at three-revolution intervals. The one-way data in run RL3 had a higher measurement noise and so produced less accurate results, but the SBDC accurately estimated the clock errors.

Run EG2 was done with a clock simulation model that included a random term added to the frequency bias, which, in this case, was set to a mean of zero and a standard deviation of 1×10^{-11} s/s. This additional error source did reduce the estimation accuracy. In addition, the effect of using the NASA standard transponder is shown in run EG3, in which the errors, as in run SG3, were unacceptably large.

Effect of Anomalous Data

The attempts to use the EKF or SBDC data editing criteria with one-way data were unsuccessful. The delta-range bias produced by the clock frequency drift gave residuals large enough to cause the estimators to delete large portions of the data sets and to diverge.

Effect of Poor Tracking Geometry

The tracking pattern used for the two-way Landsat-D case, SL1, also was tried with the SBDC and the EKF. The SBDC became unstable with such use. When used with the NASA standard transponder and estimating b, the solve-for

parameters became correlated to a high degree, with correlation coefficients of 0.9999 and higher.

The EKF did not demonstrate such instability when used with the same data, although the results were significantly degraded. This same data spacing was tried with the accurate clock models, and two such runs are shown as SL2 and EL2. In the SBDC case, SL2, the estimator instability did not develop; the highest correlation found was on the order of 0.99.

Summary of Evaluation Results

1) The performance of the EKF estimator was similar to that of the SBDC, once it had reached an equilibrium solution. This equilibrium solution required that 6-20 h of data be processed, depending on the data contact frequency and the data type. The simple process noise covariance model used with sufficient to tune the EKF successfully to different circumstances. All estimators were capable of producing results that would satisfy data annotation accuracy requirements of 100-150 m with the nominal TDRSS data, baseline error levels, and tracking schedule.

2) The range observation accuracy is degraded by TDRSS ephemeris errors. Anomalously large ephemeris errors have the potential to increase the estimation error if the range observations are included. These errors are not present in the delta-range data.

3) If one-way data are used, the accuracy of the resulting solution is highly dependent on the accuracy of the onboard modeling of the reference frequency standard. For all estimators, modeling the standard's errors as a constant bias in frequency was not sufficient when the frequency standard was simulated to be that of the NASA standard transponder. It was sufficient when a high-precision clock was substituted for the frequency standard.

4) In general, estimator performance was not degraded significantly when a few data passes were deleted.

5) When anomalous data passes were introduced, no significant increase in errors was obtained when the data were edited. Data sets were deliberately created in which the errors produced observation residuals at the borderline of the editing capability. When the anomalous errors were not detected by the editing schemes and the data processed, significant increases in the estimation errors were seen.

Conclusions

The emphasis of this study was on learning where the estimation process would fail, and whether or not one class of estimators would exhibit superior stability or other performance characteristics as the errors were increased or data frequency decreased. The primary conclusion to be drawn from this sudy is that the extended Kalman filter and the differential correction techniques performed similarly when given similar data. If a simulated problem with the data was of such severity so as to cause one of the estimators to fail, the other also could be seen to fail.

Acknowledgments

This paper was adapted from Ref. 11 and reports on work performed under NASA Contract NAS 5-24300. The authors wish to thank Dr. B. Fang for the many helpful discussions on this study.

References

[1] Waligora, S.R., "Automated Orbit Determination System (AODS) Requirements Definition and Analysis," Computer Sciences Corp., Silver Spring, Md., Rept. CSC/TM-80/6233, Sept. 1980.

[2] Long, A.C. and Gural, P.S., "Onboard Orbit Determination with Tracking and Data Relay Satellite System (TDRSS) Data, Vol. 1: Extended Kalman Filter (EKF) Evaluation," Computer Science Corp., Silver Spring, Md., Rept. CSC/TM-80/6176, Oct. 1980.

[3] Preiss, K.A. and Dunham, J.B., "Onboard Orbit Determination with TDRSS Data, Vol. 2: Sliding Batch Differential Corrector (SBDC) Evaluation," Computer Sciences Corp., Silver Spring, Md., Rept. CSC/TM-80/6234, Dec. 1980.

[4] Dunham, J.B., Long, A.C., Gural, P.S., Preiss, K.A., and Sielski, H.N., "Analysis of Estimation Algorithms for Autonomous Navigation with TDRSS Data," *Proceedings of the Fifth Annual Flight Mechanics/Estimation Theory Symposium,* NASA CP 2152, Oct. 1980, Paper 8.

[5] Nakai, Y., Smart, D.G., Morse, B.C., Koehler, R.D., and Schaffman, M.J., "Goddard Trajectory Determination System Research and Development (GTDS R&D) User's Guide," Computer Sciences Corp., Silver Spring, Md., Rept. CSC/TM-82/6005, May 1982.

[6] Dunham, J.B., "The Research and Development Goddard Trajectory Determination System (R&D GTDS) Filter Program Software Specification and User's Guide," Computer Sciences Corp., Silver Spring, Md., Rept. CSC/SD-79/6032, Dec. 1978.

[7] Cappellari, J.O., Velez, C.E., and Fuchs, A.J., "Mathematical Theory of the Goddard Trajectory Determination System," NASA Goddard Space Flight Center, Rept. X-582-76-77, April 1979.

[8] Tapley, B.D., "Statistical Orbit Determination Theory," *Recent Advances in Dynamical Astronomy,* edited by B.D. Tapley and V. Szebehely, D. Reidel, Boston, 1973, pp. 369-425.

[9] GSFC Networks Directorate, Tracking and Data Relay Satellite System User's Guide," Satellite Tracking and Data Network (STDN) Rept. 101.2, Rev. 3, Jan. 1978.

[10] Blair, B.E., "Time and Frequency Theory and Fundamentals," National Bureau of Standards Monograph 140, 1974.

[11] Van Dierendonck, A.J., Russell, S.S., Kopitzke, E.R. and Birnbaum, U., "The GPS Navigation Message," *Global Positioning System,* edited by P.M. Janiczek, Institute of Navigation, Washington, D.C., 1980, pp. 55-73.

[12] Kolenkiewicz, R. and Fuchs, A.J., "An Overview of Earth Satellite Orbit Determination, AIAA Paper 79-107, AAS/AIAA Astrodynamic Specialist Conference, Provincetown, Mass., 1979.

[13] Lerch, F.J. et al., "Gravitational Field Models of the Earth (GEM 1 and 2)," NASA Goddard Space Flight Center, Rept. X-553-72-146, May 1972.

[14] Wagner, C., Lerch, F.J., Brownd, J.E., and Richardson, J.A., "Improvement in Geopotential Derived from Satellite and Surface Data (GEM 7 and 8)," *Journal of Geophysical Research,* Vol. 82, 1977, pp. 901-914.

[15] Lerch, F.J., Klosko, S.M., Laubscher, R.E., and Wagner, C.A., "Gravity Model Improvement Using GEOS-3 (GEM 9 and 10)," NASA Goddard Space Flight Center, Rept. X-921-77-246, 1977.

[16] Dunham, J.B., Long, A.C., Preiss, K.A., Sielski, H.M., and Shenitz, C., "Algorithms for Onboard Orbit Estimation with Tracking and Data Relay Satellite System Data," Paper AIAA 81-0204, AAS/AIAA Astrodynamics Specialist Conference, Lake Tahoe, Nev., Aug. 1981.